Proteasome Regulator Marizomib (NPI-0052) Exhibits Prolonged Inhibition, Attenuated Efflux, and Greater Cytotoxicity than Its Reversible Analogs

Amanda Obaidat, Jeffrey Weiss, Brett Wahlgren, Rama R. Manam, Venkat R. Macherla, Katherine McArthur, Ta-Hsiang Chao, Michael A. Palladino, G. Kenneth Lloyd, Barbara C. Potts, Salvatore J. Enna, Saskia T. C. Neuteboom, and Bruno Hagenbuch

Departments of Pharmacology, Toxicology, and Therapeutics (A.O., B.W., S.J.E., B.H.) and Molecular and Integrative Physiology (S.J.E.), University of Kansas Medical Center, Kansas City, Kansas; University of Kansas Cancer Center, Kansas City, Kansas (B.H.); and Nereus Pharmaceuticals, Inc., San Diego, California (J.W., R.R.M., V.R.M., K.M., T.-H.C., M.A.P., G.K.L., B.C.P., S.T.C.N.)

Received December 6, 2010; accepted February 7, 2011

ABSTRACT

The present study was undertaken to compare the cellular transport characteristics of [^{3}H]NPI-0052 (1R,4R,5S)-4-(2-chloroethyl)-1-((S)-((S)-cyclohex-2-enyl)(hydroxy)methyl)-5-methyl-6-oxa-2-azabicyclo[3.2.0]heptane-3,7-dione (marizomib; salinosporamide A) and [^{3}H]NPI-0047 (1R,4R, 5S)-1-((S)-((S)-cyclohex-2-enyl)(hydroxy)methyl)-4-ethyl-5-methyl-6-oxa-2-azabicyclo[3.2.0]heptane-3,7-dione in RPMI 8226 multiple myeloma and PC-3 prostate adenocarcinoma cells to determine whether these properties explain differences in the cytotoxic potencies of these chemical analogs. The results indicate that marizomib, which possesses a chemical-leaving group, is more cytotoxic to both cell lines and inhibits proteasome activity more completely at lower concentrations than NPI-0047, a nonleaving-group analog. Moreover, it was found that both compounds accumulate in these cells by simple diffusion and the same carrier-mediated transport system. Although the rate of uptake is similar, the cellular efflux, which does not seem to be mediated by a major ATP-binding cassette (ABC)-efflux transporter, is more rapid for NPI-0047 than for marizomib. Experiments revealed that the irreversible binding of marizomib to the proteasome is responsible for its slower efflux, longer duration of action, and greater cytotoxicity compared with NPI-0047. The discovery that major ABC transporters of the multidrug resistance-associated protein family do not seem to be involved in the accumulation or removal of these agents suggests they may not be affected by multidrug resistance mechanisms during prolonged administration.

Introduction

Proteasome inhibitors such as bortezomib (PS-341, Velcade) represent a new class of anticancer agents. They induce cell death by proteasome inhibition. The 26S proteasome is an ATP-dependent multienzyme complex that is responsible for the regulated degradation of the majority of cellular and nuclear proteins, including those involved in cellular proliferation, differentiation, apoptosis, and oncogenesis (Adams, 2004). It is comprised of a 20S catalytic core particle (CP) and one or two 19S regulatory caps responsible for protein recognition and proteasome entry. The 20S CP consists of 28 subunits, including three pairs of proteolytic β subunits. These pairs are classified as chymotrypsin-like (CT-L; β5), caspase-like (β1), and trypsin-like (β2) based on their preference for cleaving substrates after hydrophobic, acidic, or basic residues, respectively (Bochtler et al., 1999; Kisselev et al., 2003). The utility of bortezomib for treating relapsed/refractory multiple myeloma (MM) and mantle cell lymphoma validates the proteasome as a valuable therapeutic target (Hideshima and Anderson, 2002; Chauhan et al., 2005b; Kane et al., 2007). Although the clinical response to bortezomib is positive, multiple toxicities and drug resistance limit its long-term use (Anderson, 2004).

A

NPI-0052: R = CH₂CH₂Cl
NPI-2151: R = CH₂CH₂OTosyl
NPI-2150: R = CH₂CH₂OMesyl
NPI-2063: R = Methyl
NPI-0047: R = Ethyl
NPI-2080: R = Propyl
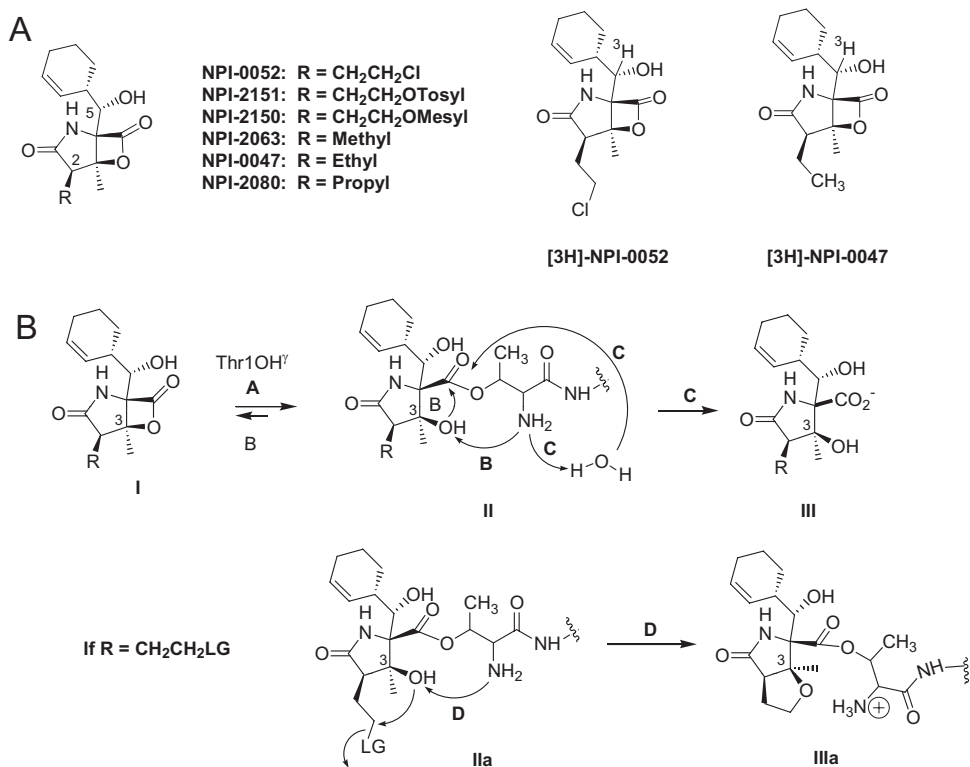
[3H]-NPI-0052   [3H]-NPI-0047

B

Fig. 1. Structures of marizomib and its analogs and mechanism of proteasome inhibition. A, marizomib and analogs with structural modifications at the C-2 substituent (R) are shown. LG compounds include marizomib (NPI-0052), NPI-2151, and NPI-2150 (LG = Cl, OTosyl, and OMesyl, respectively). NLG analogs (NPI-2063, NPI-0047, and NPI-2080) are substituted with unbranched aliphatic side chains. Structures of [³H]marizomib (NPI-0052) and [³H]NPI-0047 show the position of the tritium label at C-5. B, mechanism for reversible and irreversible inhibition of the proteasome by NLG and LG analogs, respectively. The β-lactone of the ligand (I) acylates the proteasome Thr1O$^\gamma$ (pathway A), giving rise to adduct of general structure II. In the case of NLG analogs, the ligand can be removed from the active site by Thr1NH₂-catalyzed reformation of the β-lactone ring (pathway B) or hydrolysis of the ester (pathway C); the latter pathway gives rise to deactivated product III. Cumulatively, proteasome activity is restored, i.e., inhibition is slowly reversible. In the case of LG analogs (adduct IIa, r = CH₂CH₂LG), Thr1NH₂-catalyzed nucleophilic displacement of the LG by C-3O gives stable adduct IIIa (pathway D), which is irreversibly bound.

The search for safer and more effective proteasome inhibitors has yielded a number of new compounds, including β-lactone-γ-lactams. Among this group is marizomib (NPI-0052; salinosporamide A) (1R,4R,5S)-4-(2-chloroethyl)-1-((S)-((S)-cyclohex-2-enyl)(hydroxy)methyl)-5-methyl-6-oxa-2-azabicyclo[3.2.0]heptane-3,7-dione (Fig. 1A) (Feling et al., 2003), a potent, orally active inhibitor of the three main proteolytic activities of the 20S proteasome (Chauhan et al., 2005a). Currently in clinical trials, marizomib differs structurally from other β-lactone-γ-lactam proteasome inhibitors by possessing chloroethyl and cyclohexenyl carbinol substitutions that influence its potency at, and selectivity for, proteasome active sites (Feling et al., 2003; Macherla et al., 2005). The crystal structure of marizomib in complex with yeast 20S CPs reveals that it is covalently bound to all proteolytic subunits through an ester linkage between the active site Thr1O$^\gamma$ and the carbonyl derived from the β-lactone (Groll et al., 2006). It has been shown that marizomib is irreversibly bound to the proteasome as a result of an intramolecular nucleophilic displacement of chloride and formation of a cyclic ether ring (Fig. 1B, adduct IIIa) (Groll et al., 2006). Structure-activity studies of marizomib analogs with substitutions

for the chlorine leaving group (LG) revealed that such compounds are more potent proteasome inhibitors in vitro and more cytotoxic to MM cells than nonleaving group (NLG) analogs (Macherla et al., 2005; Manam et al., 2008). Thus, inhibition of purified rabbit muscle proteasomes by LG analogs is robust and irreversible, whereas the response to NLG analogs is slowly reversible (Manam et al., 2008).

The present study was undertaken to compare some cellular properties of marizomib and NPI-0047 (1R,4R,5S)-1-((S)-((S)-cyclohex-2-enyl)(hydroxy)methyl)-4-ethyl-5-methyl-6-oxa-2-azabicyclo[3.2.0]heptane-3,7-dione in an attempt to define further the cytotoxic differences between LG and its NLG analogs. The results indicate that irreversible proteasome binding of the ligand is responsible for the slower efflux, longer duration of action, and greater potency of marizomib, an LG compound, relative to NPI-0047, an NLG analog. It was also found that these substituted β-lactone-γ-lactams are not substrates for major ABC transporters of the MRP family, suggesting that, unlike many other chemotherapeutics, the clinical response to these agents will not be affected by multidrug resistance mechanisms.

Materials and Methods

Materials. Human MM RPMI 8226 and prostate adenocarcinoma PC-3 cells and culture reagents were purchased from the American Type Culture Collection (Manassas, VA), and fetal bovine serum (FBS) from Hyclone Laboratories (Logan, UT). Marizomib, NPI-0047, NPI-2063 [(1R,4R,5S)-1-((S)-cyclohex-2-enyl)(hydroxy)methyl)-4,5-dimethyl-6-oxa-2-azabicyclo[3.2.0] heptane-3,7-dione], NPI-2080 [(1R,4R,5S)-1-((S)-((S)-cyclohex-2-enyl)(hydroxy)methyl)-5-methyl-4-propyl-6-oxa-2-azabicyclo[3.2.0] heptane-3,7-dione], NPI-2150 [2-((1R,4R,5S)-1-((S)-((S)-cyclohex-2-enyl)(hydroxy)methyl)-5-methyl-3,7-dioxo-6-oxa-2-azabicyclo[3.2.0] heptan-4-yl)ethyl methanesulfonate], and NPI-2151 [2-((1R,4R,5S)-1-((S)-((S)-cyclohex-2-enyl)(hydroxy)methyl)-5-methyl-3,7-dioxo-6-oxa-2-azabicyclo[3.2.0]heptan-4-yl)ethyl benzenesulfonate]were prepared as described previously (Macherla et al., 2005; Reed et al., 2007; Manam et al., 2008). Stock solutions were prepared in DMSO. Except for the β-lactone-γ-lactams, all chemicals and reagents were obtained from VWR International (West Chester, PA) or Sigma-Aldrich (St. Louis, MO).

Synthesis of [³H]Marizomib and [³H]NPI-0047. To prepare the radiolabeled species (Fig. 1A), marizomib (NPI-0052) was oxidized using Dess-Martin periodinane to the corresponding ketone, NPI-2062 [(1S,4R,5S)-4-(2-chloroethyl)-1-((S)-cyclohex-2-enecarbonyl)-5-methyl-6-oxa-2-azabicyclo[3.2.0]heptane-3,7-dione] (Macherla et al., 2005). The ³H label was incorporated at the C-5 position using an established synthetic transformation (Manam et al., 2007). In brief, [³H]NaBH₄ (5 Ci) was added to a solution of NPI-2062 (15 mg) in isopropyl alcohol (2 ml) containing 1% H₂O (20 μl). The solution was stirred at room temperature for 15 min and then quenched by the addition of 60 μl of glacial acetic acid, followed by repeated rotary evaporations in the presence of ethanol (3 × 5 ml). The desired diastereomer was obtained as the major product and purified by reversed-phase HPLC (Ultrasphere ODS, 250 × 9.6 mm; Beckman Coulter, Fullerton, CA) using a water/acetonitrile gradient. The purified product was concentrated to dryness on a rotary evaporator and dissolved in ethanol for storage at −80°C. Radiochemical purity was found to be 98.1% using analytical HPLC. The specific activity was adjusted to 5 Ci/mmol by the addition of unlabeled marizomib.

For [³H]NPI-0047 (Fig. 1A), the parent compound was oxidized using Dess-Martin periodinane and purified by silica gel flash chromatography using 25% ethyl acetate/hexane to obtain the corresponding purified C-5 ketone, NPI-2146 [(1S,4R,5S)-1-((S)-cyclohex-2-enecarbonyl)-4-ethyl-5-methyl-6-oxa-2-azabicyclo[3.2.0]heptane-3,7-dione]. Tritium was incorporated at the C-5 position following the general conditions detailed above for radiolabeling marizomib (Manam et al., 2007). In this case, [³H]NaBH₄ (1 Ci) was dissolved in water (100 μl) and added to a solution of NPI-2146 (5 mg) in tetrahydrofuran (2.5 ml). The reaction mixture was stirred at room temperature for 12 min and quenched by the addition of 100 μl of acetone. The solvents were removed by rotary evaporation, and the crude product was dissolved in water/acetonitrile/trifluoroacetic acid (8:2:0.01; 2 ml) and acetone (100 μl). The product was purified by reversed-phase HPLC (Ultrasphere ODS, 250 × 10 mm; Beckman Coulter) using a water/acetonitrile/trifluoroacetic acid gradient. The purified compound was concentrated to dryness on a rotary evaporator, dissolved in acetonitrile, concentrated to dryness, and redissolved in ethanol for storage at −80°C. Radiochemical purity was found to be 99.6% using analytical HPLC. The specific activity was adjusted to 5 Ci/mmol by addition of unlabeled NPI-0047. Radiosynthesis of both compounds from NPI-2062 and NPI-2146 was performed by GE Healthcare (Chalfont St. Giles, Buckinghamshire, UK).

Cell Culture. The RPMI 8226 cells (up to passage 20) were grown in suspension at 37°C in a humidified 5% CO₂ atmosphere in RPMI medium 1640 supplemented with 10% FBS, 100 U/ml penicillin, and 100 μg/ml streptomycin. The PC-3 adherent cells (up to passage 30) were grown in Ham's F12 medium supplemented with 10% FBS, 100 U/ml penicillin, and 100 μg/ml streptomycin.

In Vitro Cytotoxicity Assay. The cytotoxicity assays were performed using triplicate wells as described previously (Mitchell et al., 2004). In brief, PC-3 cells were plated in 96-well flat-bottomed plates and allowed to attach for 24 h at 37°C. The RPMI 8226 cells were plated in 96-well flat-bottomed plates on the day of testing. Serially diluted test agents (2 pM–20 μM) were added to the cells. A 0.25% (v/v) concentration of DMSO served as the vehicle control. The fluorimetric resazurin method (PerkinElmer Life and Analytical Sciences, Waltham, MA) was used to assess viability 48 h after addition of the test agents. The IC₅₀ values for cytotoxicity were calculated with Prism (GraphPad Software Inc., San Diego, CA) or XLFit 3.0 (ID Business Solutions Ltd., Emeryville, CA) using a sigmoidal dose response model.

Cell-Based 20S Proteasome CT-L Activity Assay. The RPMI 8226 and PC-3 cells were treated with various concentrations of test compounds for 1 h. After these exposures the cells were washed three times with ice-cold Dulbecco's phosphate-buffered saline (PBS) and then placed into lysis buffer (20 mM HEPES, 0.5 mM EDTA, and 0.05% Triton X-100, pH 7.3) on ice for 15 min. Cell lysates were cleared by centrifugation at 18,000g for 10 min at 4°C and protein concentration determined using the BCA assay kit (Thermo Fisher Scientific, Waltham, MA) according to the manufacturer's protocol. The CT-L activity of the 20S proteasome was measured using 20 μg of cell lysate and 20 μM of the peptide substrate Suc-LLVY-AMC (Boston Biochem, Cambridge, MA) in proteasome assay buffer (20 mM HEPES and 0.5 mM EDTA, pH 8.0), with a final SDS concentration of 0.035%. Fluorescence (λ_{ex} = 390 nm and λ_{em} = 460 nm) was measured every 5 min for 2 h with the Fluoroskan Ascent fluorometer (Thermo Fisher Scientific). The percentage of proteasome inhibition was calculated in comparison with activity recorded from cells exposed to DMSO only.

Suspension Cell Uptake Assay. The RPMI 8226 cells were washed twice with uptake buffer (116.4 mM NaCl, 5.3 mM KCl, 1 mM NaH₂PO₄, 0.8 mM MgSO₄, 5.5 mM D-glucose, and 20 mM HEPES, pH adjusted to 7.4 with Trizma base) by centrifugation at 450g for 5 min. For transport experiments the pellets were resuspended in uptake buffer at 3 × 10⁶ cells/ml. Cellular uptake was measured at 37°C by adding 200 μl of uptake buffer containing radiolabeled substrates to an equal volume of the buffer-containing cells. The assay was terminated by adding 3 ml of ice-cold uptake buffer, followed immediately by filtration through a Whatman (Clifton, NJ) GF/A filter. The filters were washed four times with 2 ml of ice-cold uptake buffer. Radioactivity retained on the filters was quantified by liquid scintillation spectroscopy (Research Products International, Mt. Prospect, IL). To correct for nonspecific filter binding, negative controls with no cells were included in all experiments and the amount of radioactivity detected in these samples was subtracted from the cellular uptake values.

Suspension Cell Efflux Assay. For efflux studies, RPMI 8226 cells were prepared in uptake buffer at a density of 3 × 10⁶ cells/ml, as was done for uptake experiments. The cells were incubated with radiolabeled substrate for 10 min and then centrifuged at 450g for 2 min. The pellets were resuspended in efflux buffer (116.4 mM NaCl, 5.3 mM KCl, 1 mM NaH₂PO₄, 0.8 mM MgSO₄, 5.5 mM D-glucose, and 20 mM HEPES, pH adjusted to 7.4 with Trizma base), and 200-μl aliquots were taken at each time point. Each aliquot was diluted with ice-cold buffer, filtered, and washed, and radioactivity was quantified as above.

Uptake and Efflux Experiments with Adherent PC-3 Cells. Uptake into PC-3 cells was performed as described previously (Gui et al., 2008). For efflux, cells on 24-well plates were exposed to the radiolabeled compounds for the indicated times, washed with warm (37°C) uptake buffer, and overlaid with 1 ml of the buffer. At the end of the efflux period the buffer was removed, and the cells were washed four times with ice-cold uptake buffer. Cells were lysed with 1% Triton X-100, and the liberated radioactivity was quantified by liquid scintillation spectroscopy (Gui et al., 2008).

TABLE 1
Cytotoxicity of LG and NLG analogs against RPMI 8226 and PC-3 cells

Compound	R	IC$_{50}$ Value ± S.D.	
		RPMI 8226	PC-3
		nM	
Marizomib (NPI-0052)	CH$_2$CH$_2$Cl	10 ± 3	35 ± 9
NPI-2150	CH$_2$CH$_2$OMesyl	144 ± 46	203 ± 46
NPI-2151	CH$_2$CH$_2$OTosyl	27 ± 9	54 ± 10
NPI-0047	Ethyl	20,000 ± 4000	16,000 ± 3000
NPI-2063	Methyl	8500 ± 3000	28,000 ± 14,000
NPI-2080	Propyl	6300 ± 3000	15,000 ± 3000

Washout Experiments. RPMI 8226 and PC-3 cells were exposed to concentrations of marizomib or NPI-0047 known to yield 50 to 70% proteasome inhibition. The PC-3 cells were seeded in tissue culture medium in six-well plates and allowed to adhere overnight. The next day, medium was replaced with tissue culture medium containing 4 nM marizomib or 1 μM NPI-0047. After a 1-h incubation at 37°C the medium was aspirated, the cells were washed once with PBS, and fresh tissue culture medium was added without test agents. The cells were placed back into the incubator and then harvested after various periods of incubation. Cell lysates were prepared and 20S proteasome CT-L activity was determined as above. The RPMI 8226 cells were suspended in tissue culture medium containing 4 nM marizomib or 10 μM NPI-0047. After 1-h incubation at 37°C the cells were collected by centrifugation (5 min at 450*g*), washed once with PBS, and resuspended in fresh tissue culture medium without test agents. The cells were placed back into the incubator and then harvested after various periods of incubation. One-milliliter portions of the cell suspension were collected by centrifugation (5 min at 450*g*), cell lysates were prepared, and 20S proteasome CT-L activity was determined.

Data Analyses. Data were analyzed using Sigmaplot (Systat Software, Inc., San Jose, CA), Prism, and Instat3 (GraphPad Software, Inc.). Kinetic constants were calculated using the Michaelis-Menten equation. The level of significance for differences between means was determined using the two-tailed unpaired Student's *t* test or Bonferroni's multiple comparison test.

Results

Cytotoxicity of LG and NLG Analogs. Previous work with the MM cell line RPMI 8226 demonstrated that LG analogs are more cytotoxic than NLG analogs (Macherla et al., 2005). To extend these findings to other cancer cells, cytotoxic activities were examined with PC-3 cells, a prostate adenocarcinoma cell line, and the results were compared with those obtained with RPMI 8226 cells. These experiments revealed that the LG analogs (NPI-0052, NPI-2150, and NPI-2151) are more potent cytotoxic agents than NLG analogs (NPI-0047, NPI-2063, and NPI-2080) against both cell types (Table 1). As shown, the IC$_{50}$ values ranged from 10 to 203 nM for the LG compounds, compared with 6 to 28 μM for the NLG analogs.

Evaluation of Proteasome Inhibition by LG and NLG Analogs in RPMI 8226 and PC-3 Cells. To examine whether the cytotoxicity is related to proteasome inhibition, the effect of LG and NLG agents on proteasome activity was determined in RPMI 8226 and PC-3 cell lines. Although marizomib is known to inhibit all three 20S proteasome activities in vitro and in vivo, only CT-L activity was measured in this study because it is the most sensitive to marizomib. Exposure to 10 to 50 nM concentrations of LG compounds resulted in >90% inhibition of CT-L activity, whereas 1 to 10 μM concentrations of the NLG analogs were required to achieve a similar inhibition in both cell lines (Fig. 2). Overall, the relative CT-L inhibitory potencies of these LG and NLG analogs are similar to their cytotoxic IC$_{50}$ values in
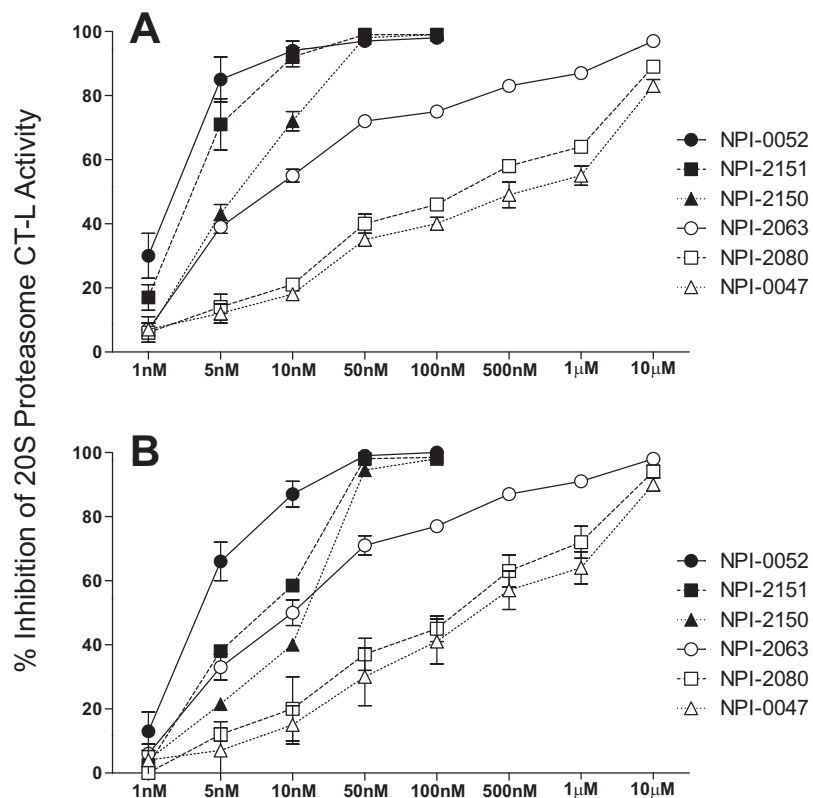
Fig. 2. Proteasome inhibition in tumor cells by LG and NLG analogs. RPMI 8226 (A) and PC-3 (B) cells were incubated with various concentrations of LG [marizomib (NPI-0052), NPI-2150, NPI-2151; filled symbols] or NLG (NPI-0047, NPI-2063, NPI-2080; open symbols) analogs for 1 h. Percentage of inhibition of CT-L activity was calculated relative to the amount of proteasome activity in cells exposed to the DMSO vehicle only. The results represent the means ± S.D. of three independent experiments, except for NPI-2150 and NPI-2151 in PC-3 for which the average of two independent experiments is shown.

Fig. 3. Characterization of marizomib and NPI-0047 uptake into RPMI 8226 and PC-3 cells. Time-dependent uptake of 10 nM [³H]marizomib ([³H]NPI-0052) (A and C) or [³H]NPI-0047 (B and D) was determined at 37°C in the absence (●) or presence of 200 nM unlabeled marizomib (▲) or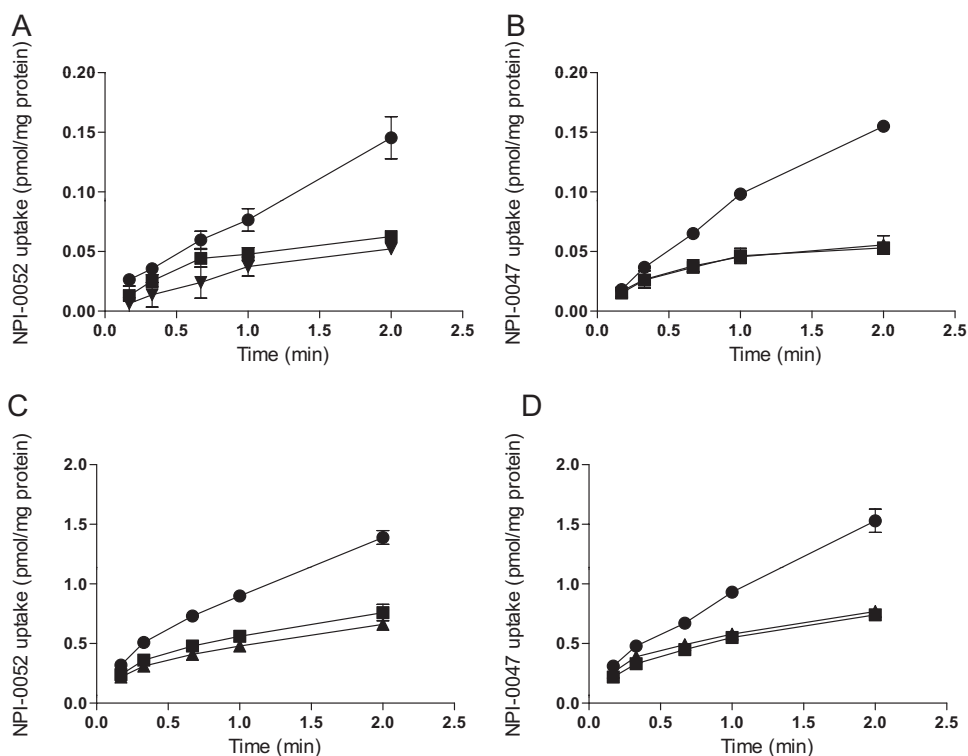 200 nM unlabeled NPI-0047 (■) in RPMI 8226 (A and B) and PC-3 (C and D) cells. Values are means ± S.E.M. of the combined values of two to three experiments performed in triplicate.

these cells (Table 1), with the LG compounds being some 1000-fold more potent than the NLG agents.

Characterization of [³H]Marizomib and [³H]NPI-0047 Uptake into RPMI 8226 and PC-3 Cells. A possible reason for the large differences in cytotoxic activities between the LG and NLG agents might be that LG analogs are more efficiently transported into cells than NLG analogs. To examine this, the uptake of [³H]marizomib and its NLG deschloro congener [³H]NPI-0047 was assessed and compared in RPMI 8226 and PC-3 cells (Fig. 3). The tritium incorporated at the C-5 position (Fig. 1A) should be stable based on the known degradation pathways for these compounds (Macherla et al., 2005; Williams et al., 2005; Denora et al., 2007). Moreover, crystal structures of marizomib and NPI-0047 in complex with the yeast 20S proteasome indicate that the C-5 position is unmodified upon ligand binding to the target (Groll et al., 2006).

The time-dependent uptake of these radiolabeled compounds (10 nM) was examined in the absence and presence of 200 nM unlabeled marizomib and NPI-0047 (Fig. 3). Both tritiated compounds were accumulated by RPMI 8226 cells in a time-dependent manner, with this uptake being inhibited to a similar degree by either unlabeled marizomib or NPI-0047 (Fig. 3, A and B). These findings suggest these two

compounds enter the cells by both diffusion and a similar saturable transport mechanism. Similar results were obtained with PC-3 cells (Fig. 3, C and D), with uptake being approximately 10 times higher than in RPMI 8226 cells (Fig. 3, A and B).

To further characterize the carrier-mediated portion of [³H]marizomib and [³H]NPI-0047 uptake, the kinetics of accumulation were assessed during the initial linear portion of uptake. Because a portion of the uptake was not saturable, the data were fitted to the Michaelis-Menten equation with the addition of a diffusional component (Table 2). The results indicate that [³H]marizomib is transported into both cell types with similar K_m and V_{max} values. However, the diffusional component was approximately 70-fold higher for PC-3 than for RPMI 8226 cells. The same experiments with NPI-0047 (Table 2) demonstrated that, as with marizomib, the K_m and V_{max} values for NPI-0047 were in the same range for both cell types. In this case the diffusional component was approximately 25-fold higher in PC-3 than in RPMI 8226 cells.

Efflux of [³H]NPI-0047 and [³H]Marizomib from RPMI 8226 and PC-3 Cells. Cells were incubated for 10 min with 20 nM of one or the other radiolabeled compounds. After this, the cells were transferred to fresh medium with-

TABLE 2
Uptake characteristics of marizomib and NPI-0047 in RPMI 8226 and PC-3 cells
Total uptake was in the absence of unlabeled inhibitor. Diffusional component was uptake in the presence of unlabeled inhibitor.

Compound	Cell Line	Uptake at 1 Min		K_m	V_{max}	Diffusional Component
		Total Uptake	Diffusional Component			
		pmol/mg protein		*μM*	*pmol/mg protein/min*	*μl/mg/min*
Marizomib	RPMI	0.08 ± 0.02	0.04 ± 0.02	0.4 ± 0.2	3.5 ± 2.1	1.4 ± 1.2
NPI-0047	RPMI	0.10 ± 0.01	0.05 ± 0.01	0.2 ± 0.3	1.1 ± 1.4	3.4 ± 1.3
Marizomib	PC-3	0.90 ± 0.06	0.48 ± 0.08	0.08 ± 0.2	3.0 ± 5.4	104 ± 9.1
NPI-0047	PC-3	0.93 ± 0.07	0.55 ± 0.06	0.03 ± 0.2	1.4 ± 4.0	91 ± 8.3

out test agent, and efflux was assessed by measuring the amount of radioactivity remaining in the cells at various times over a 2-h period. At the 2-h time point more than 80% of [³H]marizomib remained within RPMI 8226 cells, whereas the amount of [³H]NPI-0047 was less than 20% (Fig. 4A). With PC-3 cells (Fig. 4B), 75% of [³H]marizomib, but only 10% of [³H]NPI-0047, remained in the cells after the 2-h washout period.

The PC-3 cells were chosen to test whether these differences in efflux could be caused by different ABC transporters being responsible for the efflux of marizomib and NPI-0047. This cell line was used for this study because it is known to express members of the MRP family of multidrug efflux pumps (Zalcberg et al., 2000; Takeda et al., 2007). As a positive control to confirm the presence of an MRP efflux transporter, the cells were incubated for 1 h with 5 µM fluorescein, a known MRP substrate, in the absence or presence of MK-571 [3-[[[3-[(1E)-2-(7-chloro-2-quinolinyl)ethenyl]phenyl][[3-(dimethylamino)-3-oxopropyl]thio]methyl]thio]propanoic acid], a compound that inhibits MRP1 and MRP2, or probenecid or cyclosporine A, each of which inhibits a variety of ABC transporters (Sun et al., 2001). The presence of these transporters in the cells used in this study was demonstrated by the fact that at the end of the 1-h incubation period the levels of fluorescein were higher in cells incubated with the transport inhibitors (Fig. 4C). How-

ever, neither the uptake nor efflux of marizomib or NPI-0047 was affected when PC3 cells were incubated with the radiolabeled compounds in the presence or absence of ABC inhibitors (Fig. 4D). Identical results were obtained with RPMI 8226 cells (data not shown).

Persistence of Proteasome Inhibition by Marizomib and NPI-0047 in Tumor Cells. Experiments were performed to determine whether the much slower efflux of marizomib is because it is more tightly bound to intracellular constituents than NPI-0047. The persistence of proteasome inhibition by marizomib and NPI-0047 was determined by washout studies. For these experiments, PC-3 and RPMI 8226 cells were exposed for 1 h to concentrations of marizomib or NPI-0047 known to yield 50 to 70% proteasome inhibition. The cells were then washed and placed into fresh medium that did not contain either of the test agents. Cell lysates were prepared at various times during the second incubation period and proteasome activity was determined. PC-3 and RPMI 8226 cells incubated with marizomib displayed more prolonged proteasome inhibition than those exposed to NPI-0047 (Fig. 5, A and B). Cell viability was assayed in RPMI 8226 cells before they were lysed, with no differences in viability noted as a result of this period of incubation with marizomib, NPI-0047, or DMSO (Fig. 5C).
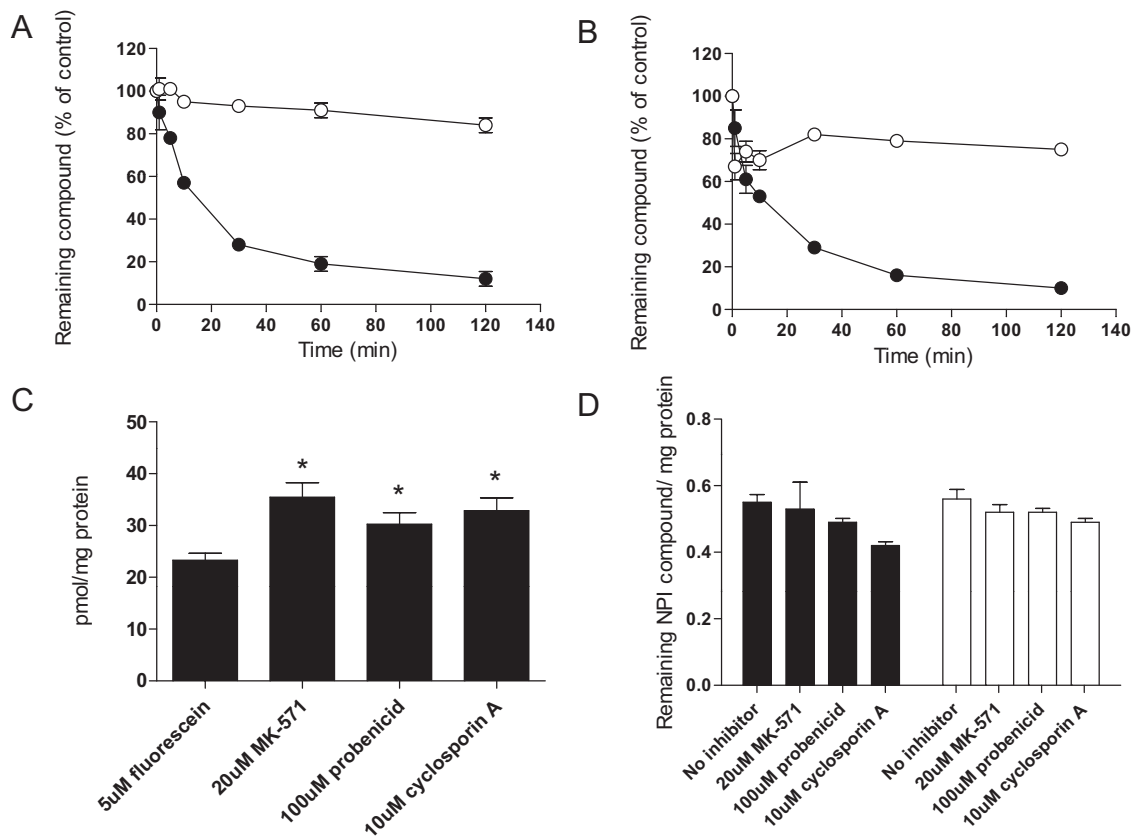

Fig. 4. Efflux of NPI-0047 and marizomib from RPMI 8226 and PC-3 cells. RPMI 8226 cells were incubated with either 20 nM radiolabeled NPI-0047 or marizomib for 10 min at 37°C. Efflux of NPI-0047 (●) and marizomib (○) was measured over 120 min after removal of the radiolabeled compounds. A and B, the data displayed in A represent the results from the RPMI 8226 study, and the PC-3 data are displayed in B. The values shown for these studies are the means ± S.E.M. of three to six experiments. C, the results obtained when PC-3 cells were incubated with 5 µM fluorescein for 1 h in the presence or absence of various concentrations of MK-571, probenecid, or cyclosporine A. D, the data obtained when PC-3 cells were incubated with 20 nM radiolabeled marizomib (filled bars) or 20 nM radiolabeled NPI-0047 (open bars) in the absence or presence of ABC efflux transporter inhibitors. The results shown for these studies are the means ± S.E.M. of the combined values from two to three experiments, each of which was performed in triplicate. ∗, $P < 0.05$.
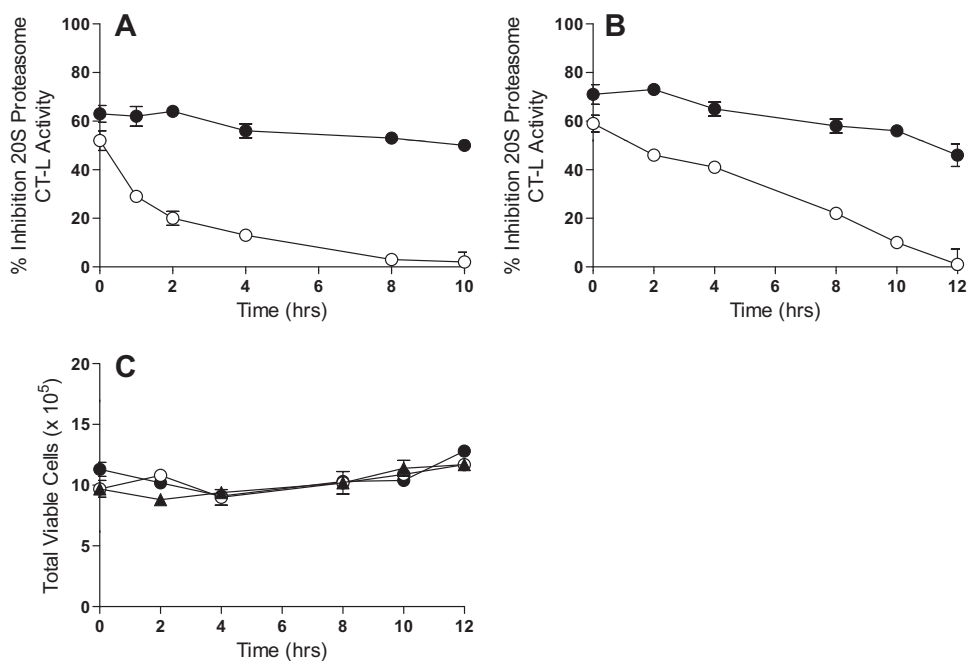
Fig. 5. Recovery of proteasome CT-L activity after removal of the test agents. Tumor cells were treated with marizomib (●), NPI-0047 (○), or DMSO (▲) for 1 h, after which the cells were washed and incubation was continued in fresh medium without drug. At the indicated times, cells were lysed and CT-L activity was determined. Percentage of inhibition was calculated relative to the amount of proteasome activity in cells treated only with DMSO (0.1% v/v). A, PC-3 cells treated with 4 nM marizomib or 1 μM NPI-0047. B, RPMI 8226 cells treated with 4 nM marizomib or 10 μM NPI-0047. C, RPMI 8226 cell viability was assessed before cell lysis.

Discussion

The results of this investigation indicate that low concentrations of marizomib bind irreversibly to the proteasome in tumor cells, causing prolonged inhibition of proteasome activity. In contrast, proteasome activity is slowly restored after exposure to NPI-0047, consistent with the reversibility of its binding. It seems, therefore, that irreversible proteasome binding of marizomib, rather than differences in cellular uptake or efflux, explains its greater potency compared with NPI-0047.

This conclusion is supported by recent findings that NLG analogs, which are covalently bound to the proteasome via an ester linkage to Thr1O$^\gamma$ (Fig. 1B, adduct II), are slowly removed from the proteolytic sites by either reformation of the β-lactone ring (Fig. 1B, pathway B) or aqueous hydrolysis (Fig. 1B, pathway C), with steric interference by C-3O attenuating the latter (Groll et al., 2006, 2009; Manam et al., 2008). These competing pathways for cleaving the inhibitor-proteasome ester linkage are catalyzed by the free N terminus (Thr1NH$_2$). In the case of marizomib and other LG analogs, LG elimination from adduct IIa (Fig. 1B, pathway D) occurs more rapidly than pathways B and C, resulting in a highly stabilized adduct (Fig. 1B, adduct IIIa). The β-lactone ring is unable to reform, because C-3O is confined within the cyclic ether ring, and aqueous hydrolysis is limited by steric interference by C-3O, together with a catalytically inactivated (protonated, at least temporally) N terminus (Thr1NH$_3^+$). As a result, marizomib and other LG analogs become irreversibly bound (Groll et al., 2006, 2009; Manam et al., 2008).

One of the drawbacks of treatment with bortezomib is the development of resistance (Anderson, 2004). Because the results of the present study demonstrate that neither marizomib nor NPI-0047 are substrates for ABC-efflux pumps in either RPMI 8226 or PC-3 cells, it is unlikely that resistance will develop to this chemical class because of overexpression of these transporters.

The present findings also indicate that cellular accumulation of marizomib and NPI-0047 results from both carrier-mediated transport and simple diffusion. The kinetic data suggest that the same transporters are most likely involved in mediating the uptake of both compounds in these two cell lines. These findings, however, provide no information on the identity of these transporters. The kinetic analyses revealed that the chief differences between these cell types with regard to accumulation of these compounds are that the total uptake and diffusional component are greater in the PC-3 than in RPMI 8226 cells. Because the calculations were normalized per milligram of total cell protein, this difference could be caused by the compositions of the cell membranes, including variations in the lipid-to-protein ratio and the total amount of protein and/or proteasome concentration per cell. Nonetheless, these findings indicate that marizomib is capable of crossing cell membranes, and possibly epithelial barriers, by simple diffusion even in the absence of transport systems.

The doses of marizomib used clinically result in blood concentrations of 45 to 150 nM, which is at the lower end of the K_m values for the saturable components. The large difference in the diffusional component between the RPMI 8226 and the PC-3 cells suggests that the relevance of the transport component for overall marizomib uptake may be cell type-dependent. In RPMI 8226 cells at 100 nM marizomib, carrier-mediated uptake is responsible for 80%, whereas in PC-3 cells it is responsible for only 15% of the accumulated compound. Thus, the characteristic of the cell membrane that influences the diffusional component, rather than the presence of the uptake system, seems to be the determining factor in the rate of marizomib uptake at clinically relevant concentrations.

In conclusion, the results of these experiments indicate that the greater cytotoxic potency of marizomib (and presumably other LG analogs) compared with NPI-0047 (and other NLG analogs) is not caused by differences in cellular transport systems, but rather to high-affinity, irreversible binding to the proteasome. This provides an explanation for why the

cellular efflux of marizomib is much less than for NPI-0047 and why proteasome inhibition is more persistent for the former than the latter. The findings also suggest that because major ABC transporters of the MRP family are not involved in the accumulation or removal of these agents, these potential chemotherapeutics will, during prolonged administration, be less affected by multidrug resistance systems than other chemical classes of proteasome inhibitors.

Authorship Contributions

Participated in research design: Obaidat, Weiss, Manam, Macherla, McArthur, Chao, Palladino, Lloyd, Potts, Enna, Neuteboom, and Hagenbuch.

Conducted experiments: Obaidat, Weiss, Wahlgren, Manam, Macherla, McArthur, and Chao.

Performed data analysis: Obaidat, Weiss, Wahlgren, Manam, Macherla, McArthur, Chao, Palladino, Lloyd, Potts, Neuteboom, and Hagenbuch.

Wrote or contributed to the writing of the manuscript: Obaidat, Palladino, Lloyd, Potts, Enna, Neuteboom, and Hagenbuch.

References

Adams J (2004) The proteasome: a suitable antineoplastic target. *Nat Rev Cancer* **4:**349–360.

Anderson KC (2004) Bortezomib therapy for myeloma. *Curr Hematol Rep* **3:**65–66.

Bochtler M, Ditzel L, Groll M, Hartmann C, and Huber R (1999) The proteasome. *Annu Rev Biophys Biomol Struct* **28:**295–317.

Chauhan D, Catley L, Li G, Podar K, Hideshima T, Velankar M, Mitsiades C, Mitsiades N, Yasui H, Letai A, et al. (2005a) A novel orally active proteasome inhibitor induces apoptosis in multiple myeloma cells with mechanisms distinct from Bortezomib. *Cancer Cell* **8:**407–419.

Chauhan D, Hideshima T, and Anderson KC (2005b) Proteasome inhibition in multiple myeloma: therapeutic implication. *Annu Rev Pharmacol Toxicol* **45:**465–476.

Denora N, Potts BC, and Stella VJ (2007) A mechanistic and kinetic study of the β-lactone hydrolysis of Salinosporamide A (NPI-0052), a novel proteasome inhibitor. *J Pharm Sci* **96:**2037–2047.

Feling RH, Buchanan GO, Mincer TJ, Kauffman CA, Jensen PR, and Fenical W (2003) Salinosporamide A: a highly cytotoxic proteasome inhibitor from a novel microbial source, a marine bacterium of the new genus salinospora. *Angew Chem Int Ed Engl* **42:**355–357.

Groll M, Huber R, and Potts BC (2006) Crystal structures of Salinosporamide A (NPI-0052) and B (NPI-0047) in complex with the 20S proteasome reveal important consequences of β-lactone ring opening and a mechanism for irreversible binding. *J Am Chem Soc* **128:**5136–5141.

Groll M, McArthur KA, Macherla VR, Manam RR, and Potts BC (2009) Snapshots of the fluorosalinosporamide/20S complex offer mechanistic insights for fine tuning proteasome inhibition. *J Med Chem* **52:**5420–5428.

Gui C, Miao Y, Thompson L, Wahlgren B, Mock M, Stieger B, and Hagenbuch B (2008) Effect of pregnane X receptor ligands on transport mediated by human OATP1B1 and OATP1B3. *Eur J Pharmacol* **584:**57–65.

Hideshima T and Anderson KC (2002) Molecular mechanisms of novel therapeutic approaches for multiple myeloma. *Nat Rev Cancer* **2:**927–937.

Kane RC, Dagher R, Farrell A, Ko CW, Sridhara R, Justice R, and Pazdur R (2007) Bortezomib for the treatment of mantle cell lymphoma. *Clin Cancer Res* **13:**5291–5294.

Kisselev AF, Garcia-Calvo M, Overkleeft HS, Peterson E, Pennington MW, Ploegh HL, Thornberry NA, and Goldberg AL (2003) The caspase-like sites of proteasomes, their substrate specificity, new inhibitors and substrates, and allosteric interactions with the trypsin-like sites. *J Biol Chem* **278:**35869–35877.

Macherla VR, Mitchell SS, Manam RR, Reed KA, Chao TH, Nicholson B, Deyanat-Yazdi G, Mai B, Jensen PR, Fenical WF, et al. (2005) Structure-activity relationship studies of salinosporamide A (NPI-0052), a novel marine derived proteasome inhibitor. *J Med Chem* **48:**3684–3687.

Manam RR, Macherla VR, and Potts BCM (2007) Stereoselective enzymatic reduction of keto-salinosporamide to (−)-salinosporamide A (NPI-0052). *Tetrahed Lett* **48:**2537–2540.

Manam RR, McArthur KA, Chao TH, Weiss J, Ali JA, Palombella VJ, Groll M, Lloyd GK, Palladino MA, Neuteboom ST, et al. (2008) Leaving groups prolong the duration of 20S proteasome inhibition and enhance the potency of salinosporamides. *J Med Chem* **51:**6711–6724.

Mitchell SS, Nicholson B, Teisan S, Lam KS, and Potts BC (2004) Aureoverticillactam, a novel 22-atom macrocyclic lactam from the marine actinomycete *Streptomyces aureoverticillatus*. *J Nat Prod* **67:**1400–1402.

Reed KA, Manam RR, Mitchell SS, Xu J, Teisan S, Chao TH, Deyanat-Yazdi G, Neuteboom ST, Lam KS, and Potts BC (2007) Salinosporamides D-J from the marine actinomycete *Salinispora tropica*, bromosalinosporamide, and thioester derivatives are potent inhibitors of the 20S proteasome. *J Nat Prod* **70:**269–276.

Sun H, Johnson DR, Finch RA, Sartorelli AC, Miller DW, and Elmquist WF (2001) Transport of fluorescein in MDCKII-MRP1 transfected cells and mrp1-knockout mice. *Biochem Biophys Res Commun* **284:**863–869.

Takeda M, Mizokami A, Mamiya K, Li YQ, Zhang J, Keller ET, and Namiki M (2007) The establishment of two paclitaxel-resistant prostate cancer cell lines and the mechanisms of paclitaxel resistance with two cell lines. *Prostate* **67:**955–967.

Williams PG, Buchanan GO, Feling RH, Kauffman CA, Jensen PR, and Fenical W (2005) New cytotoxic salinosporamides from the marine actinomycete *Salinispora tropica*. *J Org Chem* **70:**6196–6203.

Zalcberg J, Hu XF, Slater A, Parisot J, El-Osta S, Kantharidis P, Chou ST, and Parkin JD (2000) MRP1 not MDR1 gene expression is the predominant mechanism of acquired multidrug resistance in two prostate carcinoma cell lines. *Prostate Cancer Prostatic Dis* **3:**66–75.

Address correspondence to: Bruno Hagenbuch, Department of Pharmacology, Toxicology, and Therapeutics, University of Kansas Medical Center, 3901 Rainbow Blvd., Kansas City, KS 66160. E-mail: bhagenbuch@kumc.edu